ISSN: 2633-4828 Vol. 5 No.4, December, 2023

International Journal of Applied Engineering & Technology

INCREASING EFFICIENCY AND SAFETY OF THE CHAIR MAN-RIDING SYSTEM FOR UNDERGROUND MINING

Subhodeep Bhowmick[1], Dr. Rajni Kant[2] and Pranay Moon[3]
[1]Research Scholar, Master of Technology, Mining Engineering, BIT, Ballarpur (MS), 442701
[2]Principal, Ballarpur Institute of Technology, Ballarpur District-Chandrapur (MS), 442701
[3]Assistant Professor, Department of Mining Engineering, BIT, Ballarpur (MS), 442701

ABSTRACT

Underground mining is a difficult area for miners to work. Man riding chair lift (MRCL) system is a transportation media for the people working in underground mines. Underground mines are opened in two ways: shaft sinking vertically from the surface to the coal seam and through an incline drifted horizontally following some gradient pattern normally 1:4.5 up to the coal seam. People have to travel a long distance to reach up to the working faces in underground mines through the incline. This long travelling distance consumes more time and energy to reach working places. Due to that, the miners get tired. Production losses are incurred due to less working hours and inefficiency of workers. Miners must go to the working faces by walking, which is not only time consuming but also physically demanding. MRCL is installed to facilitate the people working in underground mines. In mines, a man-rider chair lift system (MRCL) has been developed to alleviate the strain stresses caused by walking lengthy and uneven distances up to the working faces. All parameters, including horizontal and vertical distances, variation and inclination of underground mines, slope forces considering the weight of persons and chair, forces acting towards return and drive unit, curves angles, power to operate, and rope safety factor, are calculated mathematically while modelling a man-rider chair lift system for both the installation and extension phases. It reduces man effort to reach the face and also saves time. Non-destructive testing of MRCL is mandatory to ensure the safety of the people. Testing and durable structure will increase the efficiency and safety of MRCL.

Keywords- Underground Mine, Man-Riding Chairlift System (MRCL), Non-destructive testing

1 INTRODUCTION

Underground coal-mining technologies are used to excavate deep-down coal seam strata in the earth. Mines are open 24 h a day, seven days a week, and progress is made using the board and pillar development approach during every coal-mining operation. The advancement of working faces lengthens the distance that miners must travel to reach their work places. This constant increase in travel distance causes fatigue among miners and reduces productive working time. A man-rider chair lift system is the solution to overcome these situations of the underground mines

A man -riding system is employed in deeper mines to aid miners in overcoming major transportation obstacles. It helps to reduce travel time without tiring out miners working in subterranean mines while also increasing output. It is a safe, quick, and pleasant method of transporting miners across long distances with uneven horizontal and vertical bends and grades. As production losses are caused by ever-longer underground travel distances, these systems have become increasingly important in modern mining. The man-rider chair lift system is an electro-hydraulic mechanism with an endless rope. The driving pulley sheave is operated by a hydraulic motor that receives flow from a hydraulic pump and is powered by an electric prime mover. The drive pulley sheave rotates on its axis and revolves the rope due to tension-induced friction between the drive pulley sheave lining and the steel wire rope. Its rope runs between the hang carrying and depression pulleys on the roof, which are maintained in place by grouted tubes at underground gallery roof. The man-riding chairs are securely held on an endless wire rope by positive friction. Roller stations set at regular intervals guide the wire rope itself. The wire rope is driven at the appropriate speed by a drive station located at the system's head.

The embarking and disembarking stations are used to pick up and drop off riders as well as to ensure reliable chair uncoupling and pick-up by the wire rope at the transition area from wire rope to rail. The return station and tensioning tower weight are erected at the conclusion of the transit section. Curve stations hung in the transport segment by anchoring chains can address horizontal course variations effectively. The individual rides on the MRCL in the mine use a chair to get from one location to the desired destination and back. The man-riding chairs on an infinite wire rope are held in place by positive friction. The wire is steered by rollers spaced at no more than fifteen-meter intervals. The driving station and return pulleys are securely connected to withstand forces up to the rope's minimum breaking force. A roof hanging system with a return pulley and proper rope tensioning configuration is used for the return end installation. The return end installation and tensioning column with internal tensioning weight are installed at the downhill end. It is supported by rails and is used to adjust the tensioning distance of the counterweight. This system is also equipped with many safety features such as over-travel and over-speed switch, pull cord rope and switch, pre start alarm, emergency brake, hydraulic brake, telephone and pager phones, etc.

Coal Mines Regulations, 2017, Regulation 93(6) stated that "In case the travelling distance from the incline or adit mouth or pit bottom exceeds one kilometer or the travelling is arduous, the owner, agent and manager shall provide suitable man-riding arrangement as approved by the Chief Inspector, within one year from the date of coming into force of these regulations." Therefore, a system was designed which increases the effectiveness of utilization of workmen with reducing the drudgery of walking. MRCL is a device utilizing for transporting of the workforce to mines and back. NDT is the best engineering tool for detecting a flaw or defect developing and inherently present in the system. It is an economical and time-saving procedure. On that basis, the testing, safety and reliability of machines can be ensured. The efficiency of MRCL is increase and maintained for over the time period.

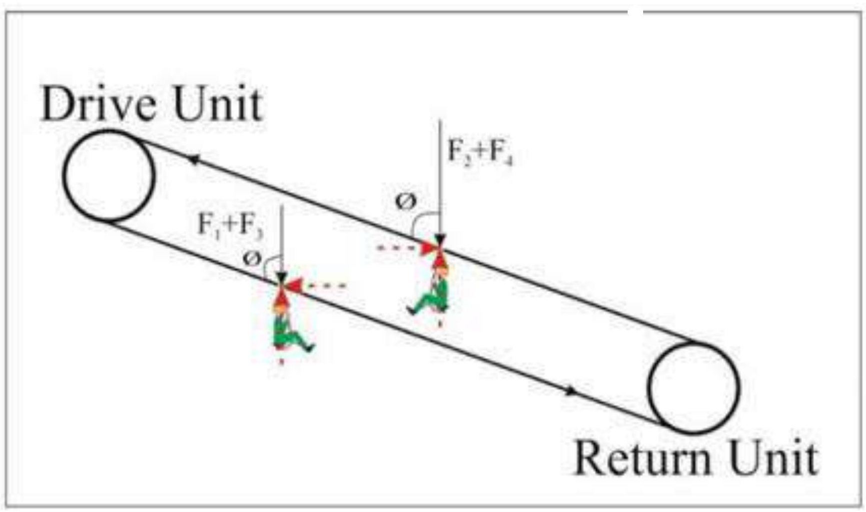

Figure 5. Forces acting on wire rope.

2 OBJECTIVE

Here there are some objectives that we are going to give a brief explanation regarding increase the efficiency and safety of the chairman-riding system for underground mining and the following objectives that we are going to addresses are:

1. To review the methodology of design and safety factor of the Man rider chair lift system.
2. To review the Non-destructive test for the durability and safety of the Man rider chair lift system. and provide the recommendation.

3 METHODOLOGY

It is critical to address risk assessment and safety during the design, installation, and extension stages of MRCL in accordance with the DGMS recommendations as per CMR Regulation 93(6). But it is importance for check the efficiency of MRCL. To relieve the strain pressures produced by travelling long and unequal distances up to the working faces in underground mines, an MRCL was devised to be installed in the mine,

3.1 Load Calculation for Man Rider

Assume, The MRCL is installed at the mines according to the IS 17242-2019. The drive head of MRCL is grouted at the pit top of the incline, and its tail end is grouted in the below-ground mine at the desired place up to the length of the installation. The distance between two tubes and two riders is 15 m.

Gradient = Ratio of one meter drop in RL to horizontal distance covered (1:X)

$\emptyset = \tan^{-1}(\text{Gradient})$

3.2 Calculation of Slope Forces

F1 and F2 are the forces resulting from the weight of persons (assumed average weight 80 kgf/pers);

F3 and F4 are the resulting forces from the weight of chairs (13 kgf/chair);

F1 and F3 are the forces acting in the direction from the drive unit to the return unit.

F2 and F4 are the forces acting in the direction from the return to the drive unit, as shown in fig.

$F_{P.D} = (80 \times 9.81 \times \text{Horizontal Distance} \times \sin\emptyset)/15$ ………. (2)

$F_{P.U} = (80 \times 9.81 \times \text{Horizontal Distance} \times \sin\emptyset)/15$ ……… (3)

$F_{C.D} = (13 \times 9.81 \times \text{Horizontal Distance} \times \sin\emptyset)/15$ ………(4)

$F_{C.U} = (13 \times 9.81 \times \text{Horizontal Distance} \times \sin\emptyset)/15$ ………(5)

Slope forces acting on the wire rope of MRCL due to the weight of riders and chairs are calculated by the Equations (2)–(5).

$F1 = \sum F_{P.D}$; $F2 = \sum F_{P.U}$; $F3 = \sum F_{C.D}$; $F4 = \sum F_{C.U}$;

Resulting slope force:

$F_H = (F1 + F2 + F3 + F4)$ ………………………………..(6)

3.3 Calculation of Man-Riding Capacity (Mc)

Travelling speed: S (m/s);

Distance between two chairs: Lc = 15 m;

$Mc = (S \times 3600)/Lc$ [Person/hour]…… …………………(7)

3.4 Calculation of Required Rope Pulling Force (FR)

Summation of the angles of all the horizontal curves of MRCL: α_H;

Summation of the angles of all the vertical curves of MRCL: α_V;

Rolling resistance of each pulley station in straight section of the installation: R_{PS};

Rolling resistance due to a rope deviation of 3°(curves, synclines, anticlines): R_θ

Resulting rolling resistance of pulley on either side:

$F_R = R_{PS} \times L/L_P + R_\theta \times (\alpha_H + \alpha_V)/3$ …………………………(8)

Required pulling force (FP):

$F_P = F_H + 2 \times F_R$ [N] ……………………………………(9)

3.5 Calculation for the Required Output of Drive Unit

The drive unit of MRCL is comprised of an electrical motor, hydraulic power pack, hydraulic motor, and drive pulley combined to drive the steel wire rope, as shown in Figure

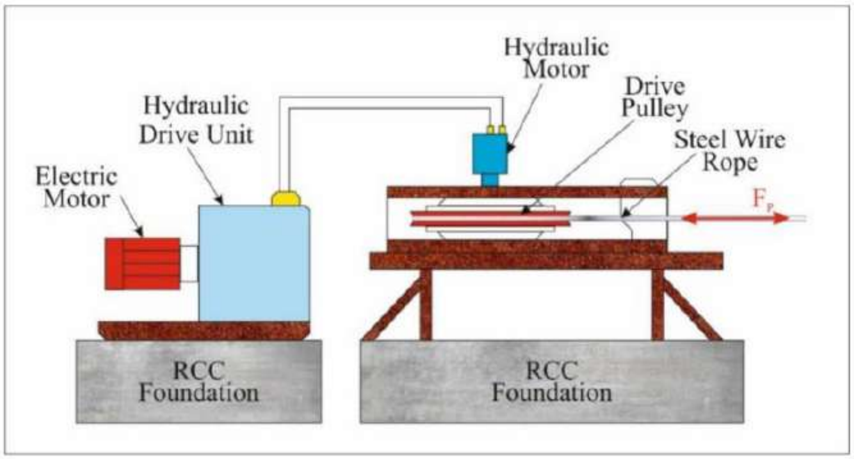

Figure 6. MRCL Drive Unit.

Required output of the drive unit (P_O):

$P_O = F_P \times S/(9.8 \times 102)$ [KW] ……………………………(10)

Efficiency of the drive unit η;

Required input of the drive unit (electric motor) (P_i):

$P_i = P_O/\eta$ [KW] …………………………………………(11)

Required capacity of induction motor = $P_i \times 1.1$ (considered factor 1.1);

Select the nearest and effective capacity of the motor to the calculated value.

3.6 Calculation of Required output of the Rope Safety F

Rope safety factor ($S.F_R$) = Ultimate strength/Working stress (F_B/F_H) must be higher than 10.

Overall maximum inclination (Average) α_m:

$\alpha_m = ((L1x\ Ø1 + L2x\ Ø2 + L3x\ Ø3 + ... + Lnx\ Øn))/L$ …....…(12)

Effective length of installation for total vertical deflection of α_m:

$L_E = L/\cos \alpha_m$ [m] ………………………………………...(13)

Maximum number of riders for the installation:

$N_R = L_E/L_C \times 2$ ……………………………………………(14)

Horizontal component of force acting on the wire rope:

$F_{HC} = F_P \times \sin 0^{\circ}$ ……………………………………......(15)

Vertical component of forces acting on suspension tubes at full capacity of the chair lift system:

$F_{VS} = ((N_R \times (W_P + W_C) \times g) + L_E \times 2 \times (W_R/100) \times g) \times \text{Cos } \alpha_m°$ [N] ……………………………………………..(16)

3.7 Calculation of Maximum Permissible Load-Bearing Capacity of Holding Bolt/Roof Bolt of Suspension Tubes

Number of suspension tubes for the total length of chairlift system:

$T = L_E/L_P$ ………………………………………… …..……(17)

Self-weight of suspension tube with carrying and depression pulley (W_{ST}):

W_{ST} = 115 kgf (approx.) …………………………………..…..(18)

Force acting on each suspension tube due to its own weight:

$F_{SS} = W_{ST} \times g$ [N] ………………………………..………(19)

Force on each suspension tube at maximum capacity of chairlift system:

$F_{ST} = F_{VS/T} + F_{SS}$ [N] ……………………………………(20)

Force on each suspension tube with two passing at the same time:

$F_{SP} = (F_{P.D} + F_{P.U} + F_{C.D} + F_{C.U}) + F_{SS} + (W_{R15} \times g \times 2)$ ……..(21)

Since $F_{SP} > F_{ST}$, we will be considering this force for calculating the load-bearing capacity of roof bolts.

Load test of each roof bolt done with minimum 5000 N;

Two roof bolts are used to fix each suspension tube, and the suspension tube arrangement is shown in Figure

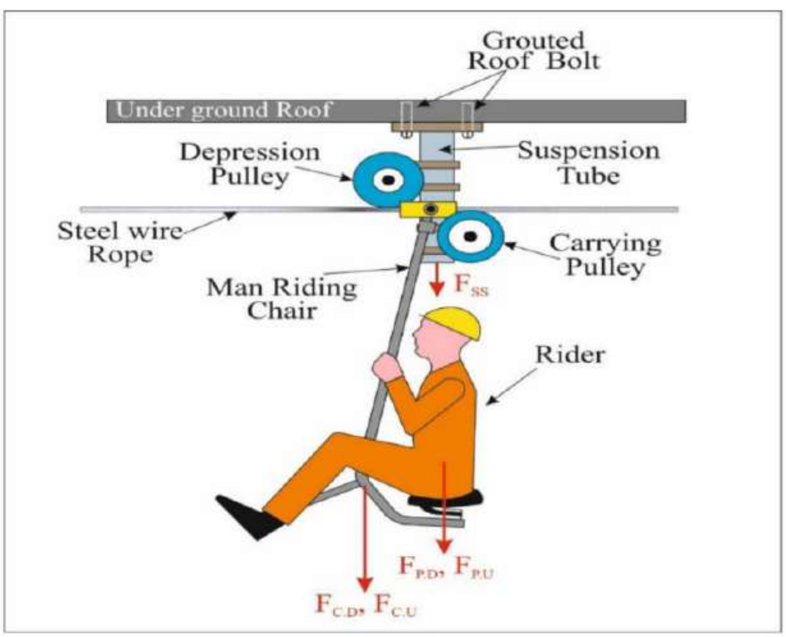

Figure 7. Suspension tube grouted with two number of roof bolt.

3.8 Factor of Safety for Each Suspension Tube

See below

$F_{ST} = 5000 \times 2/F_{SP}$ ……………………………………..(22)

3.9 Calculation of Factor of Safety of Tensioning Rope

Figure shows the rope tensioning arrangement along with counter weight.

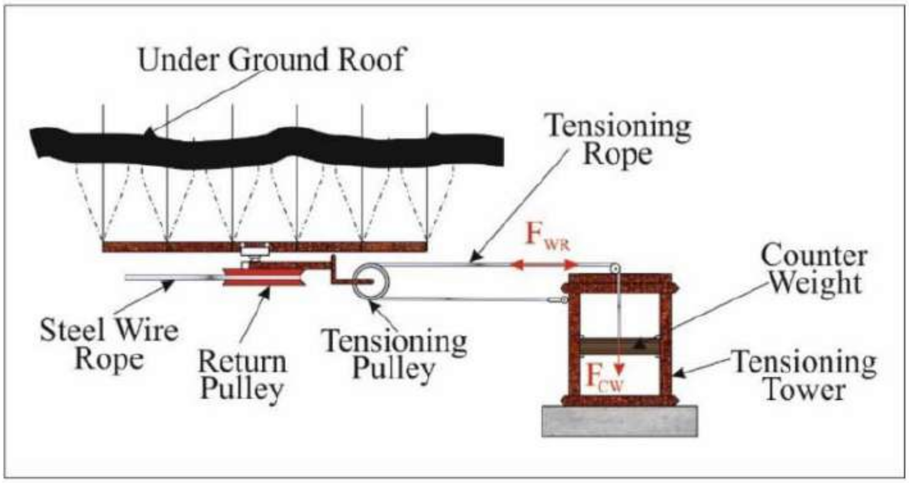

Figure 8. Rope Tensioning Unit.

Weight of counter weight W_C = 1500 kgf;

Force on tensioning rope due to counter weight:

$F_{Cw} = W_C \times 9.81$ ……………………………………..… ..(23)

Forces acting on tensioning rope:

$F_{WR} = F_{CW} + F_{HC}$ …………………………………… …(24)

Minimum breaking force of the tensioning rope B_F:

B_F = 167,000 N for 16 mm steel wire rope;

B_F = 191,000 N for 18 mm steel wire rope.

Factor of safety of tensioning rope:

$F.S_{TR}$ = Ultimate strength/Working stress = B_F/F_{WR} …… (25)

4 Requirement of rope for Man-Riding Lift Chair System

The MRCL installation and extension into two phases at underground mines. The rope should be galvanized and have a long life under typical conditions. The rope's speed should be changeable between 0 and 3 m/s. The breaking load of the rope should be at least ten times greater than the maximum static load. The time length was set at one year, and it must be assured that this rope life is not exceeded. The rope must adhere to the Indian Standard for aerial ropeways as well as the applicable clause of the Coal Mines Regulations, 2017. Table contains the technical specifications for steel wire rope. If the rope diameter falls below 10% of its original value, and there are more than 17 broken wires in a 1.5 m length or more than 8 broken wires in a 0.24 m length, the rope must be replaced.

Table 6. Steel Wire Rope Specifications.

Steel Wire Rope	Nominal Diameter	Length	Construction	Strand Construction	Tensile Grade	Type of Core	Lay Direction	Minimum Breaking Force
IS-1855/2003 (Marked)	16 mm IS 6594	Phase I—3 km Phase II—6 km	6 × 7, preformed, galvanized	6-1	1960 N/mm^2	SISAL	RHL IS 6594	16 mm^2 = 167 KN IS 1608

5 NON-DESTRUCTIVE TESTING AND TEST TECHNIQUES

Non-destructive testing of MRCL is mandatory to ensure the safety of the people and machines itself. Wahed and Farhan performed an investigation of non-destructive testing of the pressure vessel. They utilized ultrasonic flow detection and magnetic particle testing techniques for checking long seam weld and circumferential seam weld, undercuts, porosity and hairline cracks. No defect was found in the pressure vessel. Some limitations are there for checking the varying cross-sectional parts and high-current magnetizing effects in magnetic particle testing. Various cross-sectional jobs could not be tested by ultrasonic flow detection techniques. Pohl et al. investigated NDT techniques for railroad wheel and gauge corner inspection. They performed in situ inspection of rail load wheel and gauge corner especially of high-speed trains to ensure safety norms of wheels with mechanized or non-destructive inspection system. Ultrasonic wheel inspection technique and eddy current techniques were used to inspect the wheel and railway gauge corners, respectively. Gholizadeh reviewed non-destructive testing methods of composite materials. In this review study, various techniques are analyzed based on their capabilities and account their advantages and disadvantages. NDT techniques, such as visual testing, thermography, radio-graphic testing, ultrasonic testing, acoustic emission, electromagnetic testing and thermography tests, were engaged for performing these methods. These techniques are characterized based on their intrinsic characteristics and applications. Singh et al. did a review of MRCL system effectiveness in underground coal mines with reference to Ballarpur Colliery 3 and 4 pits using rank–weight method. They suggest the basic safety features to be included with the system for riskless operation of the man riders.

NDT of MRCL system was done by two methods:

(i) ultrasonic flaw detection technique

(ii) (ii) liquid dye penetration technique.

5.1 Ultrasonic Flaw Detection Technique (UFDT)

Ultrasonic flaw detection/Ultrasonic testing of a component consists of sending a beam of energy into the component. High-frequency sound energy (between 0.5 and 10 MHz) is propagating from the transducer into the testing specimen. The speed of propagation is proportional to the density and elastic behavior of the medium. Ultrasonic waves are reflected from a dissimilar surface or interface. This is the working principle of ultrasonic waves used in UFDT. The amount of reflection of ultrasonic waves from interfaces depends on the acoustic properties of the material.

Laws of light are followed by the ultrasonic waves. These waves are generated from the transducer, which transforms electrical signals to mechanical vibration and vice versa. These waves collect information and displayed on a cathode ray tube. The cathode ray tube is calibrated to enable accurate thickness measurement of locating the defect. Height, amplitude and percentage of the reflected waves are given the exact orientation and size of the defects. Figure shows the line diagram of UFDT set-up. The drive sheave pin and return pulley shafts were tested by UFDT.

Ultrasonic testing process of NDT follows the reference standard ASME Sec. V, Article 4, ASTM A609 for test procedure and ASME Sec. VIII, Div.1 Apx-12 (welding checking with angle probe) for acceptance standard. Equipment used was Digi scan DS-322 with the pulse-echo method with a light intensity of 1080 lx.

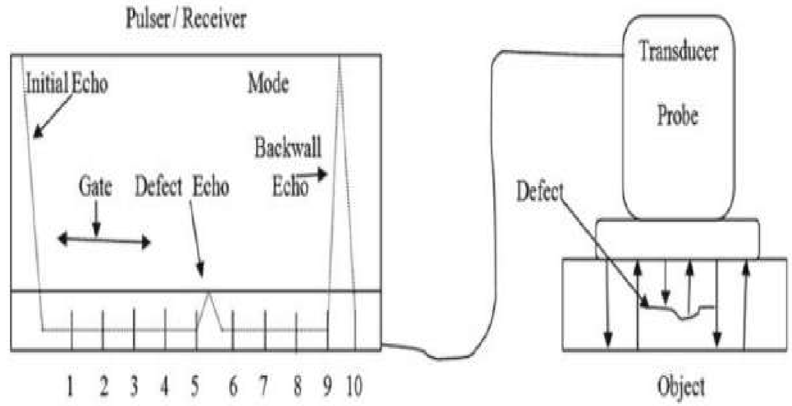

Fig. 3.2 Line diagram of UFDT set-up

5.2 Liquid Dye Penetration Testing Technique (LDPTT)

It is the most widely used non-destructive testing technique for the detection of surface flaws by a capillary phenomenon. In this NDT technique, the liquid form of penetrant is spread over the cleaned surface of the test specimen which was cleaned by cleaner or remover and waits for the next ten minutes. This liquid can be penetrated effectively in the surface discontinuities vicinity. The capillary phenomenon helps in finding the surface discontinuities, cracks and blowholes or pinhole. After ten minutes, clean the surface with cleaner and then spray the contrast colour developer on the surface. If any discontinuity is there, penetrant comes out from the vicinity of defects. Shape and size of contrast colour penetrant show the intensity of defects or cracks.

Liquid dye penetrant test process of NDT follows the reference standard ASME Sec.V, Article-24, SE-165 (IS3658-1999) for test procedure and ASME Sec. VIII, Div.1Apx.8 for acceptance standard. The light intensity is of 1080 lx.

6 CONCLUSION

The MRCL system is a man-riding arrangement designed to move workers in and out of underground mines. It is an endless machine that uses two pulleys, drive and return, to rotate steel wire rope. Curve, carrying, and depression pulleys are used to guide and support the rope of the MRCL installation all the way along its length. As a result of the rope rotating over them, these pulleys are constantly in motion when the MRCL is operating. The steel wire rope must be operated at or above FOS 10 to comply with safety regulations. The minimum breaking strength of a 16 sq mm steel wire rope is 167 KN, and the rope can only be operated with slope forces as high as 16.7 KN. The steel wire rope must be replaced after one year of continuous usage consisting of a minimum of 12 h a day, i.e., $12 \times 365 = 4380$ h, or every 10% reduction in the original cross-sectional area, whichever comes first. The strength of the steel wire rope decreases as its cross-sectional area decreases, and the impact of the practically resulting slope forces increases as the rope length and angles increase. Both occurrences reduce the factor of safety below ten, which violates the safety norms established by DGMS for the use of steel wire rope in the MRCL. Risk assessment while using the MRCL is negligible, and it is safe for operation for miners while going in and out and to and from the mines.

The novel aspect of this research is that the load was computed mathematically for each and every load-bearing portion of the MRCL. For both stages, a simulation model of steel wire was examined under the established stresses under loading conditions. This study can aid in the resolution of real-world issues involving the consideration of safety factors for design requirements that include stress and strength characteristics.

Non-destructive testing conducted on MRCL to ensure whether load bearing components are in intact condition and safe for the operation of transportation of people in the underground, both level and gradient of mines. UFDT and LDPT are conducted as an NDT of MRCL. Result of these tests ensures for continuing the use of MRCL for transporting miners in underground mines for the further next six months. Few limitations are there in ultrasonic testing procedure of NDT. We cannot test the material which unable to transmit ultrasound waves. Thickness, permeability, grained structure and shape of the material to be tested can create difficulty in ultrasonic testing. Thin size, course- grained structure and irregular shapes' components are difficult to check by ultrasonic method of NDT testing. The orientation of the defects concerning the sound beam, size, nature and distribution of the defects within the test material can affect the ability to detect the flaws. Large surface area test piece can consume more time for testing, and therefore, this technique is expensive. Highly skilled and experienced manpower is required to conduct the UFDT as compared with other methods of NDT.

7 RECOMMENDATIONS

To increase the efficiency, safety and life of MRCL, we should follow the Indian Standard for aerial ropeways as well as the applicable clause of the Coal Mines Regulations, 2017. For design, used above mentioned methodology as per the requirements. Over design of MRCL will also reduce the efficiency and safety. We should follow the all the related codes, standard and safety rules for the design and operation. Before the use of MRCL, we should conduct NDT testing as per relevant standards and codes for safety purpose.

NDT test will most important for check the durability and strength. Safe design and strength will increase the efficiency of MRCL. For safety, we should conduct the testing every 6 month of uses of MRCL. And changes and modification will done every one years of uses of MRCL.

8 REFERENCE

1. Siddiqui, M.; Pal, S.K.; Dewangan, N.; Chattopadhyaya, S.; Sharma, S.; Nekoonam, S.; Issakhov, A. Sludge Formation Analysis in Hydraulic Oil of Load Haul Dumper 811MK V Machine Running at Elevated Temperatures for Bioenergy Applications. Int. J. Chem. Eng. 2021, 2021, 4331809.
2. Siddiqui, M.A.H.; Chattopadhyaya, S.; Sharma, S.; Assad, M.E.H.; Li, C.; Pramanik, A.; Kilinc, H.C. Real-Time Comprehensive Energy Analysis of the LHD 811MK-V Machine with Mathematical Model Validation and Empirical Study of Overheating: An Experimental Approach. Arab. J. Sci. Eng. 2022, 47, 9043–9059.
3. Siddiqui, M.A.H.; Akhtar, S.; Chattopadhyaya, S.; Sharma, S.; Assad, M.E.H.; Singh, J.; Aggarwal, V.; Dwivedi, S.P.; Saxena, A. Investigation of geo-mining green roof seismic energy balancing with resin bolting by Universal Drilling Machine: A novel energy-absorbing-based support system. Arab. J. Geosci. 2022, 15, 431.
4. Siddiqui, M.A.H.; Agrawal, A.K.; Chattopadhyaya, S. In Situ Non-destructive Testing of Man Riding Chair Lift System. In Proceedings of International Conference in Mechanical and Energy Technology; Springer: Singapore, 2020.
5. Iphar, M.; Cukurluoz, A.K. Fuzzy risk assessment for mechanized underground coal mines in Turkey. Int. J. Occup. Saf. Ergon. 2020, 2, 256–271.
6. Niczyporuk, Z.T. Safety management in coal mines—Risk assessment. Int. J. Occup. Saf. Ergon. 1996, 2, 243–250.
7. Feyrer, K. Wire Ropes; Springer: Berlin/Heidelberg, Germany, 2007.
8. Peterka, P.; Krešák, J.; Kropuch, S.; Fedorko, G.; Molnar, V.; Vojtko, M. Failure analysis of hoisting steel wire rope. Eng. Fail. Anal. 2014, 45, 96–105.

9. Singh, R.; Mallick, M.; Verma, M. Studies on failure behaviour of wire rope used in underground coal mines. Eng. Fail. Anal. 2016, 70, 290–304.

10. Chang, X.-D.; Huang, H.-B.; Peng, Y.-X.; Li, S.-X. Friction, wear and residual strength properties of steel wire rope with different corrosion types. Wear 2020, 458–459, 203425.

11. Sousa, R.A.; Varela, M.L.R.; Alves, C.; Machado, J. Job shop schedules analysis in the context of industry 4.0. In Proceedings of the 2017 International Conference on Engineering, Technology and Innovation: Engineering, Technology and Innovation Management Beyond 2020: New Challenges, New Approaches, ICE/ITMC 2017-Proceedings, Madeira, Portugal, 27–29 June 2017.

12. Arrais-Castro, A.; Varela, M.L.; Putnik, G.; Ribeiro, R.; Machado, J.; Ferreira, L. Collaborative framework for virtual organisation synthesis based on a dynamic multi-criteria decision model. Int. J. Comput. Integr. Manuf. 2018, 31, 857–868.

13. Canadas, N.; Machado, J.; Soares, F.; Barros, C.; Varela, L. Simulation of cyber physical systems behavior using timed plant models. Mechatronics 2018, 54, 175–185.

14. Campos, J.C.; Machado, J.; Seabra, E. Property patterns for the formal verification of automated production systems. In Proceedings of the IFAC Proceedings Volumes (IFAC-Papers Online), 17(1 PART 1), 17th World Congress, International Federation of Automatic Control, IFAC, Seoul, Korea, 6–11 July 2008.

15. Kunz, G.; Machado, J.; Perondi, E.; Vyatkin, V. A Formal Methodology for Accomplishing IEC 61850 Real-Time Communication Requirements. IEEE Trans. Ind. Electron. 2017, 64, 6582–6590.

16. Zhiqian, R.; Xun, C. Research on fatigue life of steel wire ropes under impact loads based on double Pareto lognormal distribution. Adv. Mech. Eng. 2017, 9, 1–7.

17. Wang, S.; Liu, F.; Du, Y.; Meng, G. Stress analysis and life improvement of steel wire rope under bending process. Mech. Ad-Vanced Mater. Struct. 2020, 28, 1–10.

18. Beltrán, J.F.; Nuñez, E.; Nuñez, F.; Silva, I.; Bravo, T.; Moffat, R. Static response of asymmetrically damaged metallic strands: Experimental and numerical ap-proach. Constr. Build. Mater. 2018, 192, 538–554.

19. Giglio, M.; Manes, A. Life prediction of a wire rope subjected to axial and bending loads. Eng. Fail. Anal. 2004, 12, 549–568.

20. Guerra-Fuentes, L.; Torres-López, M.; Hernandez-Rodriguez, M.; Garcia-Sanchez, E. Failure analysis of steel wire rope used in overhead crane system. Eng. Fail. Anal. 2020, 118, 104893.

21. Wahid, A.; Mouhib, N.; Ouardi, A.; Sabah, F.; Chakir, H.; Elghorba, M. Experimental prediction of wire rope damage by energy method. Eng. Struct. 2019, 201, 109794.

22. Xue, S.; Shen, R.; Shao, M.; Chen, W.; Miao, R. Fatigue failure analysis of steel wire rope sling based on share-splitting slip theory. Eng. Fail. Anal. 2019, 105, 1189–1200.

23. Webber-Youngman, R.C.W.; van Heerden, G.M.J. Engineering principles for the design of a personnel transporta-tion system. J. S. Afr. Inst. Min. Metall. 2016, 116, 441–454.

24. Van Heerden, G.M.J. Engineering Principles for the Design of a New/Existing Mine's Personnel Transportation System (Case Study BafokengRasimone Platinum Mine). Ph.D. Thesis, University of Pretoria, Pretoria, South Africa, 2014.

25. Coal Mines Regulation 2017.pdf-160 The Gazette Of India: Extraordinary [Part Ii-Sec. 3(I)] Ministry of Labour and Employment Notification New Delhi | Course Hero. (n.d.). Available online:https://www.coursehero.com/file/52793434/Coal-MinesRegulation-2017pdf/ (accessed on 19 July 2022).

26. Ridge, I.; Chaplin, C.; Zheng, J. Effect of degradation and impaired quality on wire rope bending over sheave fatigue endurance. Eng. Fail. Anal. 2001, 8, 173–187.

27. Meksem, A.; El Ghorba, M.; Benali, A.; El Barkany, A. Optimization by the Reliability of the Damage by Tiredness of a Wire Rope of Lifting. Appl. Mech. Mater. 2011, 61, 15–24.

28. Salleh, S.; Abdullah, M.; Abdulhamid, M.; Tamin, M. Methodology for reliability assessment of steel wire ropes under fretting fatigue conditions. J. Mech. Eng. Sci. 2017, 14, 2488–2502.

29. Wessels, W. Practical Reliability Engineering and Analysis for System Design and Life-Cycle Sustainment; CRC Press: Boca Raton, FL, USA, 2010.

30. Todinov, M. Reliability and Risk Models: Setting Reliability Requirements; John Wiley & Sons: Hoboken, NJ, USA, 2015.

31. Lv, Z.; Guo, J.; Lv, H. Safety Poka Yoke in Zero-Defect Manufacturing Based on Digital Twins. IEEE Trans. Ind. Inform. 2022.

32. Zhang, C.; Mousavi, A.A.; Masri, S.F.; Gholipour, G.; Yan, K.; Li, X. Vibration feature extraction using signal processing techniques for structural health monitoring: A review. Mech. Syst. Signal Process. 2022, 177, 109175.

33. Huang, H.; Huang, M.; Zhang, W.; Yang, S. Experimental study of predamaged columns strengthened by HPFL and BSP under combined load cases. Struct. Infrastruct. Eng. 2020, 17, 1210–1227.

34. Xu, J.; Park, S.H.; Zhang, X.; Hu, J. The Improvement of Road Driving Safety Guided by Visual Inattentional Blindness. IEEE Trans. Intell. Transp. Syst. 2022, 23, 4972–4981

35. Guo, Y.; Yang, Y.; Kong, Z.; He, J.; Wu, H. Development of Similar Materials for Liquid-Solid Coupling and Its Application in Water Outburst and Mud Outburst Model Test of Deep Tunnel. Geofluids 2022, 2022, 8784398.

36. Zhu, Z.; Wu, Y.; Liang, Z. Mining-Induced Stress and Ground Pressure Behavior Characteristics in Mining a Thick Coal Seam With Hard Roofs. Front. Earth Sci. 2022, 10, 843191.

37. Zheng, W.; Zhou, Y.; Liu, S.; Tian, J.; Yang, B.; Yin, L. A Deep Fusion Matching Network Semantic Reasoning Model. Appl. Sci. 2022, 12, 3416.

38. Wang, J.; Tian, J.; Zhang, X.; Yang, B.; Liu, S.; Yin, L.; Zheng, W. Control of Time Delay Force Feedback Teleoperation System with Finite Time Convergence. Front. Neurorobot. 2022, 16, 877069.

39. Lu, S.; Ban, Y.; Zhang, X.; Yang, B.; Liu, S.; Yin, L.; Zheng, W. Adaptive control of time delay teleoperation system with uncertain dynamics. Front. Neurorobot. 2022, 16, 928863.